plants

MDPI

Article

Structural Insights into Cell Wall-Related Vesicle Secretion with Different Mechanisms

Jiawen Yang [1,2,†], Sheng Chang [3,†], Linlin Li [3], Xiaoyu Ma [1], Hua Han [3], Zheng Liu [1,2,*] and Jian Zhu [1,4,*]

1 Cryo-Electron Microscopy Center, Department of Biology, Southern University of Science and Technology, Shenzhen 518055, China; yangjw3@sustech.edu.cn (J.Y.); ma000657@umn.edu (X.M.)
2 Department of Pharmacology, School of Medicine, Southern University of Science and Technology, Shenzhen 518055, China
3 Institute of Automation, Chinese Academy of Sciences, Beijing 100190, China; changsheng2017@ia.ac.cn (S.C.); lilinlin@ia.ac.cn (L.L.); hua.han@ia.ac.cn (H.H.)
4 School of Life Sciences and Technology, Tongji University, Shanghai 200092, China
* Correspondence: liuz3@sustech.edu.cn (Z.L.); zhujian1@tongji.edu.cn (J.Z.)
† These authors contributed equally to this work.

Abstract

Exocytosis is a fundamental biological process in all eukaryotes involving the vesicular transport of cellular cargo to the plasma membrane or extracellular space. However, in walled organisms such as plants, fungi, and certain archaea, the rigid cell wall presents a unique barrier to vesicular secretion. The dense, structured matrix of the mature cell wall restricts the passage of macromolecules and vesicles, raising the fundamental question of how vesicle secretion operates in this constrained environment. In the present study, we integrate transmission electron microscopy (TEM), cryo-electron tomography (cryo-ET), and serial section electron tomography (SS-ET) to investigate the structural mechanisms underlying cell wall-related exocytosis. We demonstrate that secretory vesicles do not undergo fusion with the plasma membrane in cell wall-related vesicle secretion in *Arabidopsis thaliana* (*A. thaliana*) and *Saccharomyces cerevisiae* (*S. cerevisiae*). Furthermore, in the floral nectary of *A. thaliana*, we identify the details of vesicles inside the multivesicular body (MVB)-like structure in cell wall. Collectively, these results reveal distinct vesicle secretion pathways adapted to the presence of a cell wall, expanding our understanding of how secretory vesicles traverse and deliver cargo beyond the plasma membrane in walled eukaryotic cells.

Keywords: vesicular trafficking; cell wall-related vesicle secretion; TEM; ET

Check for updates

Academic Editor: Olga A. Zabotina

Received: 19 January 2026
Revised: 10 February 2026
Accepted: 20 February 2026
Published: 22 February 2026

Copyright: © 2026 by the authors. Licensee MDPI, Basel, Switzerland. This article is an open access article distributed under the terms and conditions of the Creative Commons Attribution (CC BY) license.

1. Introduction

Biological membranes are essential for cellular integrity and survival, defining both the cell boundary and the architecture of intracellular organelles [1]. Composed primarily of a fluid lipid bilayer [2], these membranes provide a dynamic platform for lipid–protein interactions that generate specialized domains with distinct structural and functional properties. Such domains enable critical cellular processes including energy storage, signal transduction, and compartmentalization [3–5]. Through vesicular transport, membrane-bound organelles communicate with one another via the exchange of transport vesicles [6–9]. According to the vesicular transport hypothesis, cargo transfer between organelles within the secretory pathway is mediated by discrete trafficking vesicles [10]. These vesicles undergo sequential processes, which are repeated iteratively to deliver cargo to its final intracellular

or extracellular destination. Moreover, to maintain organelle homeostasis, retrograde transport is required to return escaped resident proteins and trafficking machinery components from the acceptor compartment back to the donor compartment [6].

Endocytosis and exocytosis represent the two principal steps of vesicular trafficking, mediating bidirectional transport and communication between intracellular compartments and the extracellular environment [11]. Exocytosis is a secretory process in which trafficking vesicles deliver their cargo to the extracellular matrix by fusing with the plasma membrane, a process orchestrated by a suite of membrane fusion proteins [12]. As a fundamental mechanism in all eukaryotic cells, exocytosis not only facilitates membrane expansion but also ensures the targeted delivery of molecules to the cell surface. Two protein assemblies—the exocyst complex and the soluble N-ethylmaleimide sensitive factor attachment protein receptor (SNARE) complex—play essential roles in coordinating vesicle tethering and membrane fusion during this process [13–17].

In conventional exocytosis, intracellular vesicles fuse with the plasma membrane to release their cargo into the extracellular space, and plasma membrane homeostasis is maintained through transient fusion and compensatory membrane recycling [18]. However, in cell wall-containing organisms, such as plants, yeasts and algae, vesicle secretion may also support the synthesis, deposition, and remodeling of cell wall components and wall-modifying enzymes processes that are essential for cell wall assembly, expansion, and mechanical integrity [19]. Previous studies have demonstrated that cell wall-related vesicle secretion plays key roles not only in cell–cell communication but also in directing polarized wall growth and morphogenesis [20–23]. The rigid yet porous cell wall, therefore, presents a unique structural barrier that requires specialized strategies for exocytic vesicle delivery. To investigate these mechanisms, we integrated transmission electron microscopy (TEM), cryo-electron tomography (cryo-ET), and serial section electron tomography (SS-ET) to visualize cell wall-related vesicle secretion across diverse systems. Our observations show that the vesicles can enter and transit into the cell wall as intact structures, without undergoing classical membrane fusion. We also identified both single-vesicle and multivesicular body (MVB)-like associated exocytic pathways operating at the wall interface. Collectively, these results expand the current conceptual framework of vesicle secretion in walled cells and reveal how extracellular cargoes are mobilized to support wall growth and remodeling.

2. Results

2.1. Vesicular Trafficking with Single Vesicles in Plants

Vesicular trafficking is essential for plant growth and development, mediating the targeted delivery of newly synthesized proteins and other cargoes to organelles such as the endoplasmic reticulum, Golgi apparatus and endosomes, as well as to the plasma membrane [24,25]. To investigate cell wall-related vesicle secretion in multicellular higher plants, we analyzed the ultrastructure of *Arabidopsis thaliana* (*A. thaliana*) floral nectary prepared by high-pressure freezing followed by freeze substitution (HPF-FS) [26,27], which optimally preserves ultrastructure for TEM. Three vesicles at different stages of secretion from the Golgi apparatus were observed (Figure 1a,b). The largest vesicle entered the cell wall, the smallest remained attached a cisterna, and all vesicles exhibited progressive maturation during the secretory process. A series of exocytic events at the cell wall were captured (Figure 1c–h), providing detailed insights into how transport vesicles crossed the plasma membrane and entered the cell wall (Figure 1i). Initially, the vesicles approaching the cell wall were surrounded by a fork-like deformation of the plasma membrane (Figure 1c). Then, the termini of the fork-like plasma membrane structure fused, creating a transient double membrane that enveloped the secretory vesicle. Subsequently, the membrane layer adjacent to the vesicle disintegrated, leaving the vesicle enclosed by a single membrane

(Figure 1d). Afterwards, the cytoplasmic-facing membrane protrusion gradually flattened, restoring membrane stability, as the vesicle advanced further into the cell wall (Figure 1e,f). Finally, the transport vesicle became fully embedded within the cell wall matrix, where it was poised to participate in cell wall remodeling or secretory activities (Figure 1h).

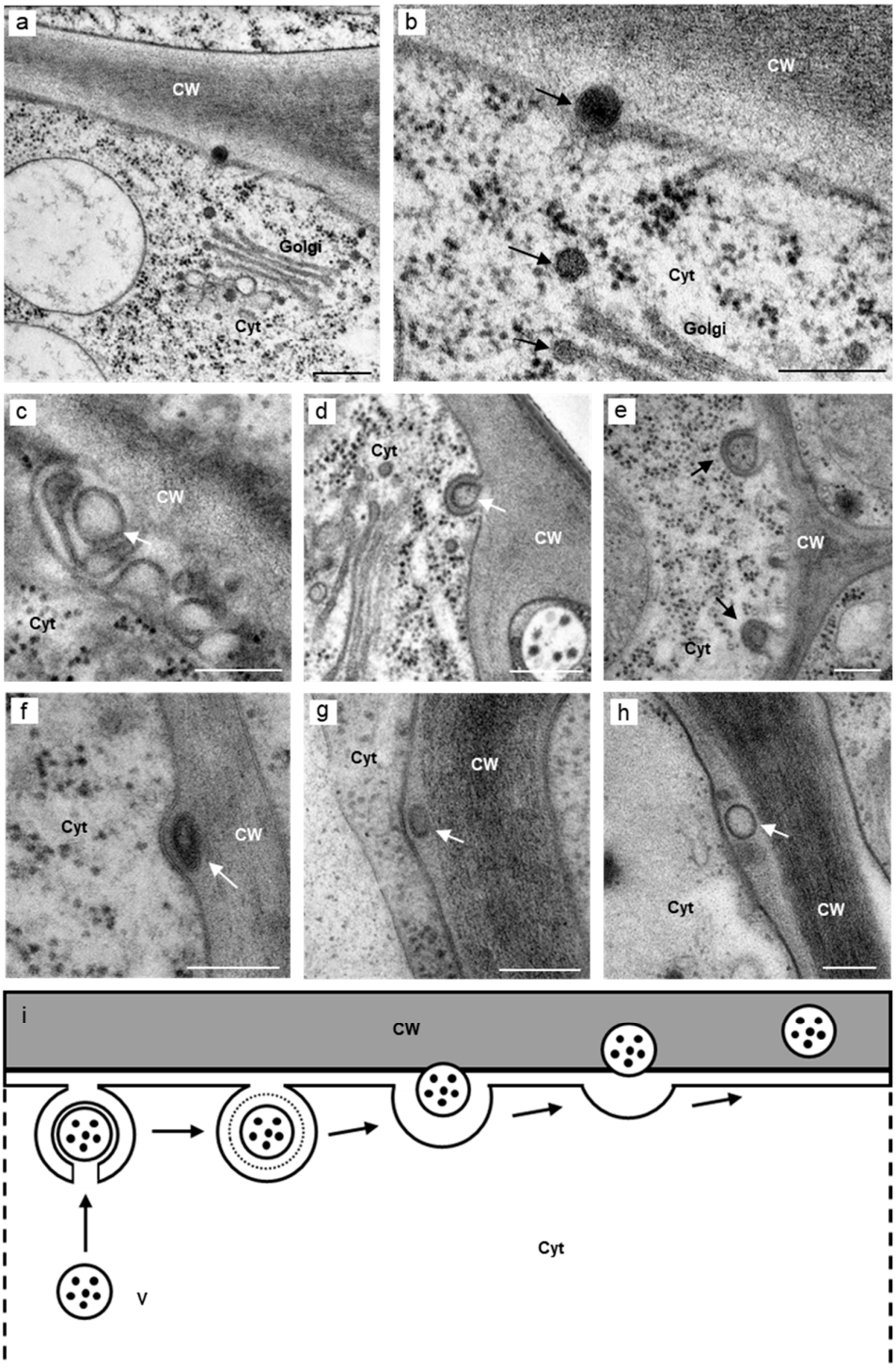


Figure 1. The process of cell wall-related vesicle secretion in *A. thaliana* floral nectary cells. (**a**) Three vesicles were breaking away from cisternae of the Golgi apparatus and the bigger vesicle had already situated in the cell wall, and the other smaller one was still connected with the cisterna. (**b**) Zoomed

view of the Golgi region in (**a**). (**c**) TEM image showing a secretory vesicle position near the cell wall, and the adjacent plasma membrane protrudes inward to form a fork-like structure whose termini are tended to enclose the secretory vesicle; the termini of the fork-like structure of the plasma membrane then fused to enclose the secretory vesicles. (**d**) The inner membrane enclosed the vesicle and disappeared, subsequently presented by the dotted line in (**i**), leaving the vesicle surrounded by the remaining outer membrane as the vesicle began to enter the cell wall. (**e**) TEM images illustrating progressive recovery of the plasma membrane to its original contour as the vesicle advances into the cell wall. (**f**–**h**) After completion of secretion, the intact vesicle resides within the cell wall matrix. (**i**) Schematic model summarizing each stage with single vesicle in cell wall-related vesicle secretion. Arrows indicate vesicles; CW, cell wall; Cyt, cytoplasm. Scale bar: 200 nm.

Notably, our observations revealed the presence of intact exocytic vesicles within the cell wall (Figure 1f,h). In our study, vesicles appeared to traverse directly into the cell wall following localized membrane remodeling. This departure from the classical fusion mechanism may arise from the unique mechanical and structural constraints imposed by the rigid cell wall. Collectively, these results suggest that organisms with rigid cell walls have evolved a distinct exocytotic pathway, one that is specifically adapted to the biological and functional requirements of the wall matrix.

2.2. Vesicular Trafficking with Multivesicular Body-like Structure in Plants

Soluble proteins lacking vacuolar sorting signals are secreted to the extracellular space via single exocytic vesicles. In contrast, those containing such signals are recognized and packaged into MVBs, which are the key intermediate compartments in the plant secretory pathway [28–30]. MVBs play a central role in cargo delivery and degradation, and their biogenesis is a well-established step in trafficking toward the vacuole or plasma membrane [31,32]. To determine whether both single vesicle and MVBs-associated routes contribute to cell wall-related vesicle secretion, we examined TEM datasets from *A. thaliana* floral nectary tissues and observed multivesicular structures positioned near the cell wall, consistent with ongoing vesicle exocytosis (Figure 2). Owing to the distinct size relative to conventional MVBs, we referred to this multivesicular structure as an MVB-like structure. TEM images captured two sequential stages of MVB-like associated exocytosis, namely Stage 1 and Stage 2. In this process, the outer membrane of the MVB-like structure fusing with the plasma membrane enabled the discharge of internal vesicles into the cell wall (Figure 2). During Stage 1, the outer membrane of the MVB-like structure fused with the plasma membrane, eliminating the inter-membrane boundary. Following this fusion, the MVB-like structure became anchored at the cell wall interface, and its internal vesicles prepared to enter the wall matrix (Figure 2a–c). By Stage 2, the internal vesicles completely entered the cell wall and plasma membrane after fusion with the outer membrane of the MVB-like structure and were recovering (Figure 2d, Video S1). These released internal vesicles may support the role of MVB-like structures derived from trafficking in cell wall-related secretion.

Our observations reveal that MVB-like structures involved in cell wall-related vesicle secretion were heterogeneous in size and number of internal vesicles. Alongside large MVB-like structures packed with internal vesicles, smaller MVB-like structures were also observed, underscoring the structural diversity within this population (Figure 2e–h, Videos S2 and S3). Using electron tomography (ET), we reconstructed the 3D architecture of these smaller MVB-like structures, allowing detailed visualization of internal vesicles organization. These reconstructions reveal that internal vesicles within a single MVB-like structure could either remain isolated or establish physical connections with one another (Figure 2f,h). This organizational flexibility suggests that upon delivery into the cell wall, internal vesicles may aggregate or coordinate their release, potentially enabling the bulk transfer of cell wall-modifying components.

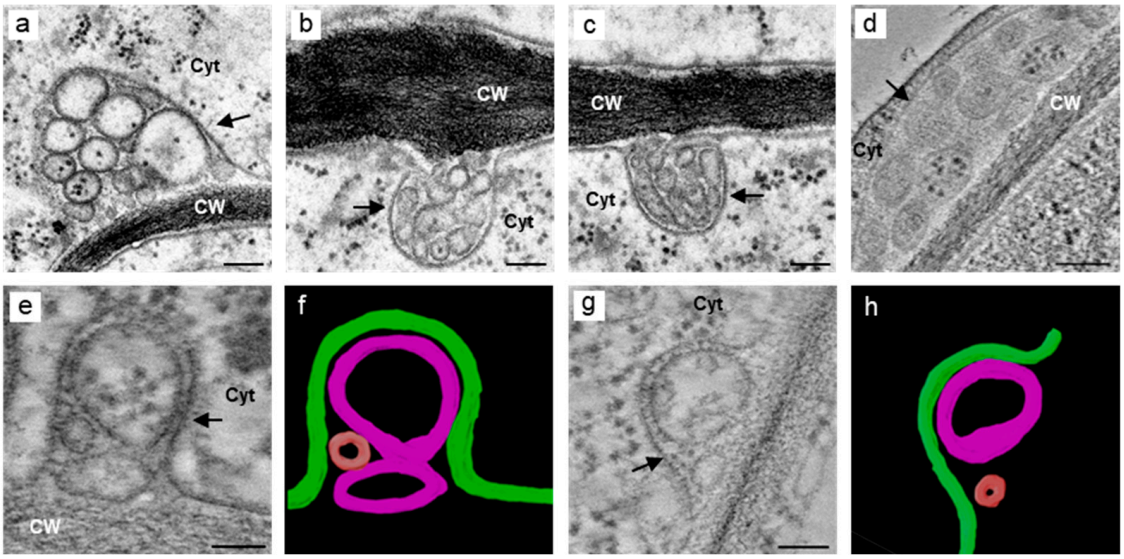


Figure 2. The transporting process of multivesicular bodies in cell wall-related vesicle secretion of *A. thaliana* floral nectary cells. (**a**–**c**) TEM images showing MVB-like structures at sequential stages of exocytosis positioned near the cell wall. (**d**) A tomographic slice capturing internal vesicles had entered the cell wall and plasma membrane recovering after fussing with the outer membrane of MVB-like structure. (**e**,**g**) Tomographic slices showing MVB-like structures embedded within the cell wall. (**f**,**h**) Segmentations of MVB-like structures shown corresponding to (**e**,**g**), respectively; the plasma membrane is pseudo-colored in green, and internal vesicles within the MVB-like structures are pseudo-colored in pink and magenta. Arrows indicate vesicles; CW, cell wall; Cyt, cytoplasm. Scale bar: 100 nm in (**a**–**d**) and 50 nm in (**e**–**h**).

Given our observation that internal vesicles can interconnect with one another, we next investigated whether these vesicles undergo fusion or fission during MVB-like associated cell wall-related vesicle secretion. To resolve the biogenesis and spatial organization of internal vesicles within secreted MVB-like structures, we performed serial section electron tomography (SS-ET) to generate near-complete 3D reconstructions of individual MVB-like structures at sequential secretion stages. Thick serial sections were manually collected, imaged independently via ET, and then aligned and merged to generate a unified reconstruction of each MVB-like structure. Analysis of one MVB-like structure across five consecutive serial sections revealed dynamic internal vesicles rearrangements during cell wall entry (Figure 3a–e, Video S4). 3D reconstruction and segmentation confirmed that the internal vesicles ultimately coalesced into a single, integrated vesicle within the MVB-like structure (Figure 3f). In the early stage of cell wall entry, the internal vesicles within MVB-like structures were mostly individual, though some contact may be seen (Figure 2); however, in later stages, after complete entry into the cell wall, a single large vesicle was observed, presumably due to the fusion of the previously separate intraluminal vesicles. These results suggest that during MVB-like associated cell wall-related vesicle secretion, internal vesicles can undergo sequential fusion events, forming a unified luminal compartment that may facilitate bulk cargo release to support cell wall growth. Based on these results, we propose that during cell wall-related vesicle secretion, MVB-like structures undergo a coordinated series of internal vesicle fusion events coupled with outer membrane remodeling within the MVB-like structure. This mechanism likely promotes efficient release of cell wall-modifying components, thereby facilitating wall biogenesis and expansion.

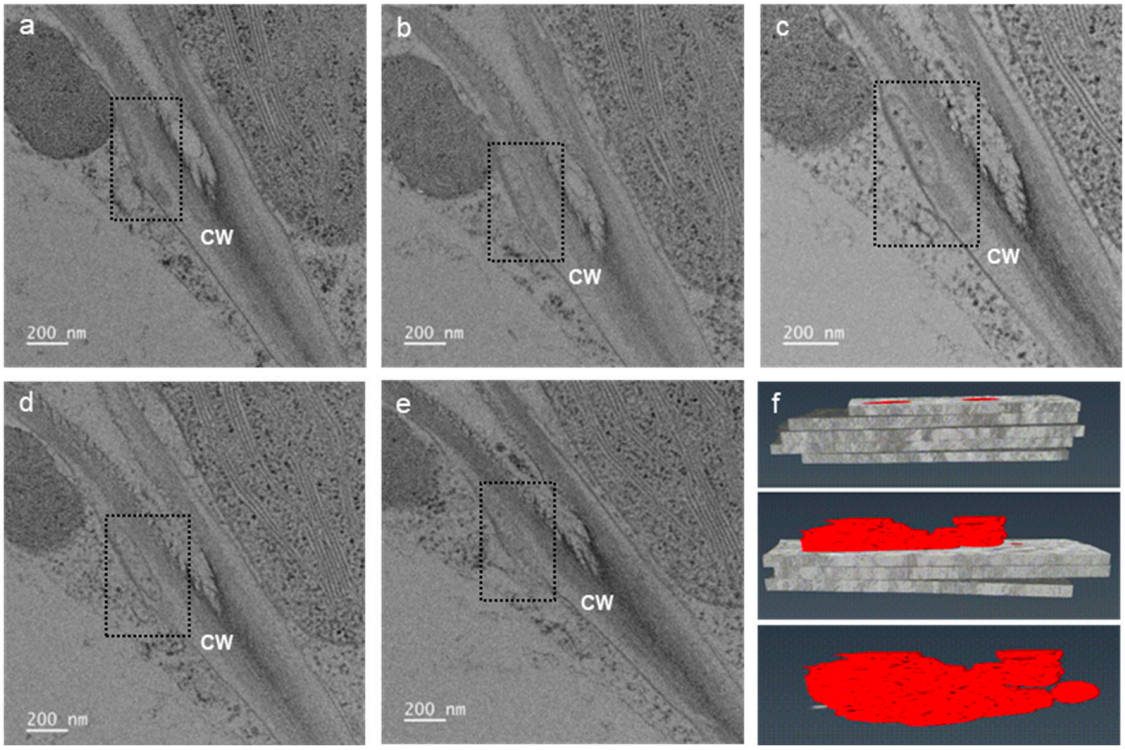


Figure 3. Serial-section electron tomography of MVB-like associated cell wall-related vesicle secretion in *A. thaliana*. (**a**–**e**). TEM images from five consecutive serial sections showing internal vesicles exocytosed to the cell wall; internal vesicles are labeled by black dash boxes. (**f**) 3D reconstructions generated from the five serial tomograms depicting the ultrastructure and spatial organization of the internal vesicles within the MVB-like structure. The large, integrated vesicle indicated in red may form by the fusion of individual internal vesicles within MVB-like structure. Scale bar: 200 nm.

2.3. Transporting Vesicles in the Yeast Cell Wall

The yeast *Saccharomyces cerevisiae* (*S. cerevisiae*) possesses a characteristic two-layered cell wall architecture, consisting of a microfibrillar inner layer that provides mechanical strength and a brush-like outer layer rich in mannoproteins [33,34]. To investigate how secretory vesicles cross this barrier, we prepared yeast cells using HPF-FS. TEM images revealed multiple vesicles located outside the plasma membrane, presumably en route to or already embedded within the cell wall matrix (Figure 4a). Notably, one vesicle with a distinct membrane was observed containing electron-dense material matching the cytoplasmic composition. This morphological continuity indicated that the vesicle originated in the cytoplasm and was transported intact into the cell wall.

We next utilized cryo-focused ion beam milling (cryo-FIB) combined with cryo-ET to visualize the three-dimensional (3D) architecture of *S. cerevisiae* cells in a native state, thereby avoiding artifacts associated with chemical fixation (Figure 4b–f). Using this approach, we observed intact transport vesicles containing cytoplasmic material embedded within the cell wall (Figure 4b–d, Videos S5 and S6). In several tomograms, the vesicle appeared tethered to the plasma membrane just prior to its release into the wall matrix (Figure 4b, Video S5), suggesting a sequential, non-fusogenic export mechanism. Based on these observations, the cell wall-related vesicle secretion appeared to proceed through the budding of fully intact vesicles, which subsequently migrate into and accumulate within the cell wall. Detached vesicles were frequently found accumulated in the cell wall, indicating a potential vesicle reservoir that may support localized wall expansion (Figure 4c,d, Video S6). Additionally, structures resembling early endocytic intermediates were captured during the small bud growth stage, characterized by invaginated containers

with cell wall-like material (Figure 4e,f), suggesting that cell wall-related vesicle secretion may also operate through a comparable membrane deformation mechanism.

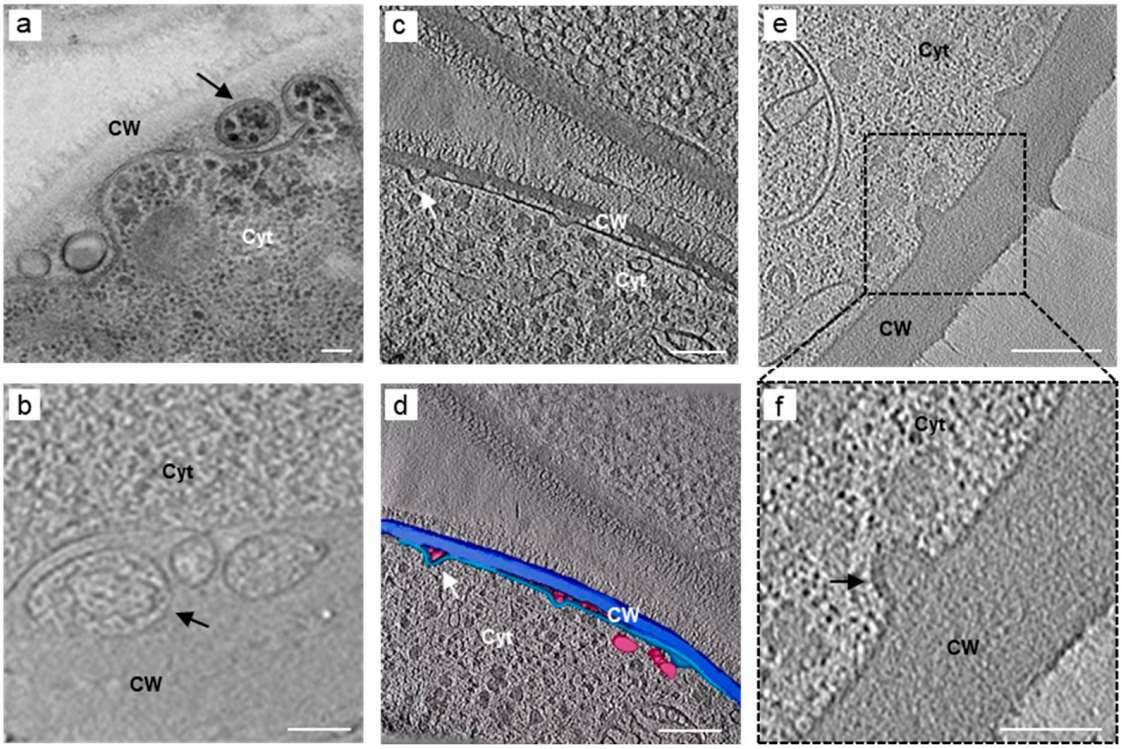


Figure 4. Transporting vesicles presenting within the *S. cerevisiae* cell wall. (**a**) TEM image of a yeast cell showing an intact vesicle within the cell wall. (**b**) A tomographic slice focusing on the region of cell wall, showing the vesicle entering the cell wall in a budding manner. (**c**) A tomographic slice showing multiple transporting vesicles accumulated within the cell wall. (**d**) Segmentation of (**c**); the cell wall is colored in blue and the vesicles are colored in pink. (**e**) A tomographic slice capturing a vesicle budding event at the cell wall, indicative of cell wall-related endocytosis. (**f**) Zoomed view of the boxed region in (**e**), showing a vesicle enclosed by a wall-derived invagination. Arrows indicate vesicles; CW, cell wall; Cyt, cytoplasm. Scale bar: 100 nm in (**a**,**b**,**d**,**f**); 200 nm in (**c**,**e**).

3. Discussion

Exocytosis serves as the principal route for secreting signaling molecules and cell wall-modifying enzymes; however, its detailed mechanics in walled cells have remained challenging to resolve due to the physical barrier posed by the cell wall itself [13]. This rigid outermost layer protects the cell but also constrains the transit of secretory vesicles. With the development of techniques, TEM has become a popular tool for the structural study of cell wall-related vesicle secretion. Since EM samples prepared by conventional chemical fixation methods are prone to artificial artifacts such as biofilm shrinkage and matrix loss, low-temperature sample preparation methods such as plunge freezing and HPF are widely used to prevent samples from chemical damage in conventional sample preparation, making the ultrastructure of the cell closer to its native state [35,36]. By integrating TEM, cryo-ET, and serial ET, the key steps and structural features of cell wall-related vesicle secretion can be observed directly by EM.

In this study, we characterized the process of cell wall-related vesicle secretion with two distinct vesicle transport patterns including single vesicle and MVB-like-structure in our plant tissues; as well as budding secretion in yeast cells. In conventional exocytosis systems, typified by animal cells, vesicles fuse with the plasma membrane and discharge their contents directly into the extracellular space. Our research further illustrates vesicle

secretion associated with the cell wall and further elaborates on the difference between membrane vesicular transport associated with the cell wall and conventional exocytosis.

Recent studies have focused on the structure and functions of extracellular vesicles (EVs) in the cell wall. In plant cells, in addition to conventional protein secretion (CPS) via the endoplasmic reticulum (ER)-Golgi apparatus-trans-Golgi network (TGN)-plasma membrane pathway, there is an unconventional protein secretion (UPS) pathway mediated by exocyst-positive organelles (EXPOs) that bypasses conventional secretory organelles and drives the biogenesis of EVs in plant cells [37,38]. The EVs have been characterized and identified in the cell wall of *Arabidopsis* root border cells, and these EXPO-derived EVs may act as a potential key component of plant defense [39]. In fungal cells, the cell wall consists of an inner framework of fibrillar polysaccharides and an outer layer enriched in mannoproteins and other glycoproteins, which together confer resistance to mechanical and environmental stress [40]. Previous research in *Schizosaccharomyces pombe (S. pombe*) demonstrated that exocytic patterning—through factors such as Sec6, Syb1, and Exo70—governs the spatial geometry of polarized growth by coordinating actin cables and exocyst dynamics [20]. As central regulators of the polarized growth cascade, exocytic vesicles destined for the cell wall, actin cables, and the exocyst complex collectively shape the architecture of growth domains. Notably, exocytosis was shown to causatively determine local growth geometry by directing where and how cell wall material is deposited [20]. When integrated with these functional insights, our structural observations reinforce the tight interdependence between cell wall mechanics and cellular morphogenesis. The presence of intact vesicles embedded within the wall further suggests that cell wall-resident vesicles may contribute to the maintenance or expansion of polarized growth domains by providing a localized reservoir of secretory material.

However, the details of processes exhibit notable differences among cell wall-related vesicle exocytosis in different cells or tissues. For instance, in *A. thaliana*, Golgi-derived secretory vesicles are expelled intact through structural modifications of the plasma membrane. In the MVB pathway, however, numerous small vesicles enter the cell wall following fusion of the MVB's outer membrane [23]. In addition, yeast secretory vesicles form through budding, while diatoms utilize secretory vesicles containing silicon for cell wall formation.

In addition to transportation and secretion, cell wall-related vesicle secretion also plays important roles in defining cell growth domains, supporting longitudinal cell expansion, maintaining membrane homeostasis and mediating cell wall formation [20,22,41]. These dynamic functions may lead to different mechanisms of vesicle secretion; for example, there are cell wall-related vesicle secretion pathways mediated by single vesicles in cells with normal growth, while MVB-like structures regulating cell wall-related vesicle secretion pathways may exist in cells with vigorous growth. MVB-like-associated cell wall-related vesicle secretion is likely to exert a stronger influence on cell wall remodeling through cell wall-related vesicle secretion and supply their larger size and greater cargo capacity. Another factor contributing to the difference in vesicle secretion between cell wall and non-cell wall contexts is the role of the cell wall in cell growth and division. In unicellular yeast and multicellular algae, cell wall-related vesicle secretion may have functions on intercellular substances' transportation and information communication as well as cell wall growth, while in higher plants, cell wall-related vesicle secretion may be mainly responsible for cell wall growth, since plasmodesmata can facilitate communication and transport essential molecules between cells [20,23,41,42]. These demonstrate the unity of structures and functions.

Previous studies have proposed two main secretory mechanisms in plants including eccrine secretion and granulocrine secretion; both of the two transport modes are considered to end with membrane fusion and cargo secretion [10]. However, the intact vesicles

containing cargos are observed within the cell wall of the floral nectary tissue, indicating that secretory vesicles can enter the cell wall directly (Figure 1). This interesting cell wall-related vesicle secretion mode may be determined by the composition of the cell wall and the dependence of cargo transport. In mammalian cells or fugal cells, the coordination of membrane fusion and exocytosis mediates cargo transport, while plasmodesmata are cytoplasmic communication channels that are vital for the physiology and development of all plants [8,12,43]. The pattern of cell wall-related vesicle secretion may vary depending on the growth and developmental stages of different cells and tissues. Future studies coupling correlative light-electron microscopy with live-cell reporters and immunoelectron microscopy will be essential to explore the details of vesicles entering the cell wall and vesicle behavior afterwards.

4. Materials and Methods

4.1. Sample Preparation by High-Pressure Freezing and Freeze Substitution

Floral nectary tissue samples of *A. thaliana* were prepared by a high-pressure freezing machine (HPM-010) and freeze substitution. Yeast cell samples were cultured as previously described [44,45] and prepared using a Leica EM ICE (Leica Microsystems, Wetzlar, Germany) high-pressure freezing and a Leica EM AFS2 freeze substitution system. Briefly, samples were loaded into specimen planchettes filled with 1-Hexadecene as a cryoprotectant and rapidly frozen at −180 °C under 2100 bar high pressure. Frozen planchettes were maintained under liquid nitrogen until further processing. For optimal preservation of ultrastructure, samples were transferred into freeze substitution medium (acetone containing 2% osmium tetroxide) and placed in a Leica EM AFS2 freeze substitution system precooled to −90 °C. For freeze substitution, the samples were brought to −90 °C for 10 h and subsequently warmed to −60 °C over a period of 8 h. Then, samples were placed at −30 °C for 8 h and then 0 °C for 2 h. Following freeze substitution, samples were washed with anhydrous acetone at 0 °C and room temperature. Finally, the samples were infiltrated and embedded in Eponate 812 resin for ultrathin sectioning and TEM imaging.

4.2. EM Data Acquisition

Ultrathin (80 nm) sections of *S. cerevisiae* and *A. thaliana* prepared for TEM were imaged using a 120-kV FEI Talos L120C transmission electron microscope (Thermo Fisher Scientific, Waltham, MA, USA). Ultrathin (50 nm) sections of *A. thaliana* prepared for TEM were imaged using a 100-kV Hitach-600 transmission electron microscope (Hitachi Ltd., Tokyo, Japan).

4.3. Cryo-ET Sample Preparation

For cryo-ET grid preparation, 200 mesh holey-carbon copper grids (R2/1, Quantifoil) were glow discharged for 40 s. An aliquot of 4 μL concentrated sample of cell culture was applied to the front side of the grids, and 2.5 μL of medium was subsequently applied on the back side of the grids. Grids were back-side blotted for 5 s in a Leica EM GP2 plunge freezer (Leica Microsystems, Wetzlar, Germany) at 30 °C and 95% humidity, then vitrified by plunging into liquid ethane at −184 °C. The frozen grids were stored in sealed boxes in liquid nitrogen until further processing.

4.4. Cryo-FIB Milling

Cryo-FIB milling was performed using an Aquilos dual-beam FIB-SEM system (Thermo Fisher Scientific, Waltham, MA, USA). Cryo-EM grids were clipped into the AutoGrids in liquid nitrogen dewar and then transferred into the FIB-SEM chamber at −185 °C in a high vacuum. The samples were covered by a thick organometallic platinum

layer by a gas injection system and the milling angle was about 15°. Rough milling was performed using a 30 kV ion beam and a current of 0.3–3.0 nA, followed by fine milling at 0.1–0.3 nA. Cells were subsequently polished with an ion beam of 30–50 pA to produce lamellae with a final thickness of 100–200 nm.

4.5. Tilt Series Acquisition and Tomogram Reconstruction

Thick sections (100 nm) of *A. thaliana* prepared by HPF-FS were loaded into a JEM-F200 transmission electron microscope (JEOL Ltd., Tokyo, Japan) operating at 200 kV and equipped with a OneView camera (Gatan Inc., Pleasanton, CA, USA) for observation. Tilt images of the thin sections were acquired by a OneView camera (Gatan Inc., Pleasanton, CA, USA) at a nominal magnification of ×4000 (calibrated pixel size of 3.16 Å). The defocus range was set from −0.5 to −3 µm and the total dose was 120 $e^-/Å^2$. Tilt series were merged into one stack, aligned with patch tracking in IMOD v.4.9.12 [46] and reconstructed as back-projected tomograms with SIRT-like filtering of 5 iterations at bin2.

The lamellae of *S. cerevisiae* prepared by cryo-FIB were loaded into a 300-kV Titan Krios microscopy G3i (Thermo Fisher Scientific, Waltham, MA, USA) equipped with GIF quantum energy filter with a slit of 30 eV and a K2 Summit direct electron detector (Gatan Inc., Pleasanton, CA, USA). Tilt images were acquired by a K2 camera under super resolution mode at a nominal magnification of ×42,000 (calibrated pixel size of 3.43 Å). A dose-symmetric scheme was used to collect tilt series starting at the angle of the lamella plane while ending at ±48° (relative to the lamella plane) with an increment step of 3°, using SerialEM v.3.7. Each tilt image was recorded as a video stack consisting of 10 frames with a dose of 3.64 $e^-/Å^2$. The defocus range was set from −4 to −6 µm and the total dose was 120 $e^-/Å^2$.

Video frames of each tilt were motion corrected, summed and binned with a factor of two using MotionCor2 v.1.1.0 [47]. Tilt series were merged into one stack, aligned with patch tracking in IMOD v.4.9.12 [46], and reconstructed using back projection with SIRT-like filtering of 5 iterations at bin4.

4.6. Serial Section Electron Tomography

Eight to ten thick sections (250–380 nm) of *A. thaliana* prepared by HPF-FS were mounted onto single-slot grids coated with a Formvar film. The grid was loaded into a JEM-F200 transmission electron microscope (JEOL Ltd., Tokyo, Japan) operating at 200 kV and equipped with a OneView camera (Gatan Inc., Pleasanton, CA, USA). Following manual adjustment of focus, brightness, contrast, and astigmatism, all imaging was recorded under low-dose conditions. First, an overview image of the target structure was acquired at ×5000 magnification, followed by a high-magnification image at ×20,000 to visualize ultrastructure details. Subsequently, tilt series from −60° to +60° (at 2° increments) were collected using SerialEM v.3.7, and the tomographic reconstruction was generated using the IMOD v.4.9.12 [46].

To obtain regions of interest (ROIs) in serial section, the approximate positions of ROIs were estimated using affine transformation, based on the predictable spatial relationships between sequentially collected sections. Precise registration of consecutive ET volumes, which often have significant contrast variations, was achieved through a coarse-to-fine strategy utilizing multi-scale image feature matching followed by refinement with the Belief Propagation-Elastic (BP-Elastic) algorithm. To restore missing wedge information in ET volumes, the quantity of lost images from inter-volume pixel-value changes was estimated, followed by inpainting using a network tailored for small-sample data through interpolation pre-training and distillation learning. Final segmentation of specific ultrastructure was performed using a 3D convolutional neural network, which leverages the

volumetric context to achieve rapid and accurate segmentation across the reconstructed serial tomograms.

Supplementary Materials: The following supporting information can be downloaded at: https://www.mdpi.com/article/10.3390/plants15040660/s1, Video S1–S3: Tomogram of *A. thaliana* capturing internal vesicles in the cell wall; Video S4: Tomogram of five consecutive serial sections revealing dynamic internal vesicle rearrangements in the cell wall; Video S5: Tomogram of yeast showing the vesicle being secreted to the cell wall; Video S6: Tomogram and segmentation of yeast showing multiple transporting vesicles accumulated within the cell wall.

Author Contributions: Conceptualization, J.Z.; methodology, J.Z., J.Y., S.C., L.L. and X.M.; validation, J.Y., L.L. and J.Z.; investigation, J.Y.; data curation, J.Y., S.C. and L.L.; writing—original draft preparation, J.Y.; writing—review and editing, all authors; visualization, J.Y. and S.C.; supervision, J.Z., Z.L. and H.H.; funding acquisition, J.Z. and Z.L. All authors have read and agreed to the published version of the manuscript.

Funding: This research was funded by the National Natural Science Foundation of China (30470863 to J.Z. and 32241028 to Z.L.) and the Instrument Function Development Innovation Program of Chinese Academy of Sciences (E5J12301 to C.S.).

Data Availability Statement: The original contributions presented in this study are included in the Supplementary Material. Further inquiries can be directed to the corresponding authors.

Acknowledgments: We sincerely thank the staff at the cryo-EM center of the South University of Science and Technology for their technical support on the Cryo-EM and High-Performance Computation platforms; we sincerely thank Hongtu Ma and Yacong Wang at the Center for Microscale Connectomics of Institute of Automation in Chinese Academy of Sciences for their assistance with electron microscopy and their technical support; we sincerely thank the staff at the Lab of Electron Microscopy I of Institute of Cell Biology in ETH Zurich.

Conflicts of Interest: The authors declare no conflicts of interest.

Abbreviations

The following abbreviations are used in this manuscript:

TEM	Transmission electron microscopy
Cryo-ET	Cryo-electron tomography
SS-ET	Serial section electron tomography
MVB	Multivesicular body
SNARE	Sensitive factor attachment protein receptor
HPF-FS	High-pressure freezing followed by freeze substitution
Cryo-FIB	Cryo-focused ion beam milling
EV	Extracellular vesicle
CPS	Conventional protein secretion
ER	Endoplasmic reticulum
TGN	Trans-Golgi network
UPS	Unconventional protein secretion
EXPO	Exocyst-positive organelles
ROI	Regions of interest

References

1. Casares, D.; Escribá, P.V.; Rosselló, C.A. Membrane Lipid Composition: Effect on Membrane and Organelle Structure, Function and Compartmentalization and Therapeutic Avenues. *Int. J. Mol. Sci.* **2019**, *20*, 2167. [CrossRef] [PubMed]
2. Bloom, M.; Evans, E.; Mouritsen, O.G. Physical properties of the fluid lipid-bilayer component of cell membranes: A perspective. *Q. Rev. Biophys.* **1991**, *24*, 293–397. [CrossRef] [PubMed]

3. Escribá, P.V. Membrane-lipid therapy: A historical perspective of membrane-targeted therapies—From lipid bilayer structure to the pathophysiological regulation of cells. *Biochim. Biophys. Acta Biomembr.* **2017**, *1859*, 1493–1506. [CrossRef]
4. Karnovsky, M.J.; Kleinfeld, A.M.; Hoover, R.L.; Klausner, R.D. The concept of lipid domains in membranes. *J. Cell Biol.* **1982**, *94*, 1–6. [CrossRef]
5. van Meer, G.; Voelker, D.R.; Feigenson, G.W. Membrane lipids: Where they are and how they behave. *Nat. Rev. Mol. Cell Biol.* **2008**, *9*, 112–124. [CrossRef]
6. Bonifacino, J.S.; Glick, B.S. The mechanisms of vesicle budding and fusion. *Cell* **2004**, *116*, 153–166. [CrossRef]
7. Olkkonen, V.M.; Ikonen, E. When intracellular logistics fails—Genetic defects in membrane trafficking. *J. Cell Sci.* **2006**, *119*, 5031–5045. [CrossRef]
8. Takamori, S.; Holt, M.; Stenius, K.; Lemke, E.A.; Grønborg, M.; Riedel, D.; Urlaub, H.; Schenck, S.; Brügger, B.; Ringler, P.; et al. Molecular anatomy of a trafficking organelle. *Cell* **2006**, *127*, 831–846. [CrossRef]
9. Tanaka, N.; Kyuuma, M.; Sugamura, K. Endosomal sorting complex required for transport proteins in cancer pathogenesis, vesicular transport, and non-endosomal functions. *Cancer Sci.* **2008**, *99*, 1293–1303. [CrossRef]
10. Fahn, A. *Plant Anatomy*; Pergamon: Oxford, England, 1990.
11. Karatekin, E.; Rothman, J.E. FEBS Letters Special Issue on Exocytosis and Endocytosis. *FEBS Lett.* **2018**, *592*, 3477–3479. [CrossRef] [PubMed]
12. Augustine, G.J.; Burns, M.E.; DeBello, W.M.; Pettit, D.L.; Schweizer, F.E. Exocytosis: Proteins and perturbations. *Annu. Rev. Pharmacol. Toxicol.* **1996**, *36*, 659–701. [CrossRef]
13. Adnan, M.; Islam, W.; Zhang, J.; Zheng, W.; Lu, G.D. Diverse Role of SNARE Protein Sec22 in Vesicle Trafficking, Membrane Fusion, and Autophagy. *Cells* **2019**, *8*, 337. [CrossRef]
14. Arasaki, K.; Shimizu, H.; Mogari, H.; Nishida, N.; Hirota, N.; Furuno, A.; Kudo, Y.; Baba, M.; Baba, N.; Cheng, J.; et al. A role for the ancient SNARE syntaxin 17 in regulating mitochondrial division. *Dev. Cell* **2015**, *32*, 304–317. [CrossRef] [PubMed]
15. Hála, M.; Cole, R.; Synek, L.; Drdová, E.; Pecenková, T.; Nordheim, A.; Lamkemeyer, T.; Madlung, J.; Hochholdinger, F.; Fowler, J.E.; et al. An exocyst complex functions in plant cell growth in Arabidopsis and tobacco. *Plant Cell* **2008**, *20*, 1330–1345. [CrossRef]
16. Harrison, M.J.; Ivanov, S. Exocytosis for endosymbiosis: Membrane trafficking pathways for development of symbiotic membrane compartments. *Curr. Opin. Plant Biol.* **2017**, *38*, 101–108. [CrossRef] [PubMed]
17. TerBush, D.R.; Maurice, T.; Roth, D.; Novick, P. The Exocyst is a multiprotein complex required for exocytosis in Saccharomyces cerevisiae. *EMBO J.* **1996**, *15*, 6483–6494. [CrossRef] [PubMed]
18. Battey, N.H.; James, N.C.; Greenland, A.J.; Brownlee, C. Exocytosis and endocytosis. *Plant Cell* **1999**, *11*, 643–660. [CrossRef]
19. Hoffmann, N.; Mohammad, E.; McFarlane, H.E. Disrupting cell wall integrity impacts endomembrane trafficking to promote secretion over endocytic trafficking. *J. Exp. Bot.* **2024**, *75*, 3731–3747. [CrossRef]
20. Abenza, J.F.; Couturier, E.; Dodgson, J.; Dickmann, J.; Chessel, A.; Dumais, J.; Salas, R.E.C. Wall mechanics and exocytosis define the shape of growth domains in fission yeast. *Nat. Commun.* **2015**, *6*, 8400. [CrossRef]
21. An, Q.; Ehlers, K.; Kogel, K.H.; van Bel, A.J.; Hückelhoven, R. Multivesicular compartments proliferate in susceptible and resistant MLA12-barley leaves in response to infection by the biotrophic powdery mildew fungus. *New Phytol.* **2006**, *172*, 563–576. [CrossRef]
22. de Haan, D.; Aram, L.; Peled-Zehavi, H.; Addadi, Y.; Ben-Joseph, O.; Rotkopf, R.; Elad, N.; Rechav, K.; Gal, A. Exocytosis of the silicified cell wall of diatoms involves extensive membrane disintegration. *Nat. Commun.* **2023**, *14*, 480. [CrossRef] [PubMed]
23. Xu, S.; Qian, J.; Song, X.; Zhu, J. Localization and secretory pathways of a 58K-like protein in multi-vesicular bodies in callus of Arabidopsis thaliana. *Sci China C Life Sci.* **2008**, *51*, 827–832. [CrossRef] [PubMed]
24. Nielsen, E. The Small GTPase Superfamily in Plants: A Conserved Regulatory Module with Novel Functions. *Annu. Rev. Plant Biol.* **2020**, *71*, 247–272. [CrossRef] [PubMed]
25. Nielsen, E. Plant exocytosis: Weaving distinct pathways to the plant plasma membrane. *Mol. Plant* **2022**, *15*, 382–384. [CrossRef]
26. Al-Amoudi, A.; Norlen, L.P.; Dubochet, J. Cryo-electron microscopy of vitreous sections of native biological cells and tissues. *J. Struct. Biol.* **2004**, *148*, 131–135. [CrossRef]
27. Liu, S.; Pokrovskaya, I.D.; Storrie, B. High-Pressure Freezing Followed by Freeze Substitution: An Optimal Electron Microscope Technique to Study Golgi Apparatus Organization and Membrane Trafficking. *Methods Mol. Biol.* **2023**, *2557*, 211–223. [CrossRef]
28. Cui, Y.; Shen, J.; Gao, C.; Zhuang, X.; Wang, J.; Jiang, L. Biogenesis of Plant Prevacuolar Multivesicular Bodies. *Mol. Plant* **2016**, *9*, 774–786. [CrossRef]
29. Ruf, A.; Oberkofler, L.; Robatzek, S.; Weiberg, A. Spotlight on plant RNA-containing extracellular vesicles. *Curr. Opin. Plant Biol.* **2022**, *69*, 102272. [CrossRef]
30. Tse, Y.C.; Mo, B.; Hillmer, S.; Zhao, M.; Lo, S.W.; Robinson, D.G.; Jiang, L. Identification of multivesicular bodies as prevacuolar compartments in Nicotiana tabacum BY-2 cells. *Plant Cell* **2004**, *16*, 672–693. [CrossRef]
31. Henne, W.M.; Buchkovich, N.J.; Emr, S.D. The ESCRT pathway. *Dev. Cell* **2011**, *21*, 77–91. [CrossRef]

32. Palade, G.E. Studies on the endoplasmic reticulum. II. Simple dispositions in cells in situ. *J. Biophys. Biochem. Cytol.* **1955**, *1*, 567–582. [CrossRef]
33. Orlean, P. Architecture and biosynthesis of the Saccharomyces cerevisiae cell wall. *Genetics* **2012**, *192*, 775–818. [CrossRef]
34. Osumi, M. The ultrastructure of yeast: Cell wall structure and formation. *Micron* **1998**, *29*, 207–233. [CrossRef]
35. Bullen, A.; Taylor, R.R.; Kachar, B.; Moores, C.; Fleck, R.A.; Forge, A. Inner ear tissue preservation by rapid freezing: Improving fixation by high-pressure freezing and hybrid methods. *Hear. Res.* **2014**, *315*, 49–60. [CrossRef]
36. Yang, J.; Sui, S.F.; Liu, Z. Brain structure and structural basis of neurodegenerative diseases. *Biophys. Rep.* **2022**, *8*, 170–181. [CrossRef] [PubMed]
37. Cui, Y.; Gao, J.; He, Y.; Jiang, L. Plant extracellular vesicles. *Protoplasma* **2020**, *257*, 3–12. [CrossRef] [PubMed]
38. Wang, J.; Ding, Y.; Wang, J.; Hillmer, S.; Miao, Y.; Lo, S.W.; Wang, X.; Robinson, D.G.; Jiang, L. EXPO, an exocyst-positive organelle distinct from multivesicular endosomes and autophagosomes, mediates cytosol to cell wall exocytosis in Arabidopsis and tobacco cells. *Plant Cell* **2010**, *22*, 4009–4030. [CrossRef] [PubMed]
39. Gao, J.; Li, Y.; Zhang, S.; He, Y.; Liu, Z.; Wang, J.; Hua, J.; Chen, J.; Zhong, J.; Zhong, H.; et al. Structural and Functional Characterization of EXPO-Derived Extracellular Vesicles in Plants. *Adv. Sci.* **2026**, e06163. [CrossRef]
40. Pérez, P.; Cortés, J.C.G.; Cansado, J.; Ribas, J.C. Fission yeast cell wall biosynthesis and cell integrity signalling. *Cell Surf.* **2018**, *4*, 1–9. [CrossRef]
41. Wang, H.; Zhuang, X.; Wang, X.; Law, A.H.; Zhao, T.; Du, S.; Loy, M.M.; Jiang, L. A Distinct Pathway for Polar Exocytosis in Plant Cell Wall Formation. *Plant Physiol.* **2016**, *172*, 1003–1018. [CrossRef]
42. Bayer, E.M.; Benitez-Alfonso, Y. Plasmodesmata: Channels Under Pressure. *Annu. Rev. Plant Biol.* **2024**, *75*, 291–317. [CrossRef]
43. Sager, R.E.; Lee, J.Y. Plasmodesmata at a glance. *J. Cell Sci.* **2018**, *131*, jcs209346. [CrossRef] [PubMed]
44. Li, Z.; Chen, S.; Zhao, L.; Huang, G.; Pi, X.; Sun, S.; Wang, P.; Sui, S.F. Near-atomic structure of the inner ring of the Saccharomyces cerevisiae nuclear pore complex. *Cell Res.* **2022**, *32*, 437–450. [CrossRef] [PubMed]
45. Li, Z.; Chen, S.; Zhao, L.; Huang, G.; Xu, H.; Yang, X.; Wang, P.; Gao, N.; Sui, S.F. Nuclear export of pre-60S particles through the nuclear pore complex. *Nature* **2023**, *618*, 411–418. [CrossRef] [PubMed]
46. Kremer, J.R.; Mastronarde, D.N.; McIntosh, J.R. Computer visualization of three-dimensional image data using IMOD. *J. Struct. Biol.* **1996**, *116*, 71–76. [CrossRef]
47. Zheng, S.Q.; Palovcak, E.; Armache, J.P.; Verba, K.A.; Cheng, Y.; Agard, D.A. MotionCor2: Anisotropic correction of beam-induced motion for improved cryo-electron microscopy. *Nat. Methods* **2017**, *14*, 331–332. [CrossRef]

Disclaimer/Publisher's Note: The statements, opinions and data contained in all publications are solely those of the individual author(s) and contributor(s) and not of MDPI and/or the editor(s). MDPI and/or the editor(s) disclaim responsibility for any injury to people or property resulting from any ideas, methods, instructions or products referred to in the content.